Taylor & Francis
Taylor & Francis Group

Advanced Composite Materials

ISSN: 0924-3046 (Print) 1568-5519 (Online) Journal homepage: http://www.tandfonline.com/loi/tacm20

Characterization of poly(vinyl alcohol)/acrylamide/alkylammonium montmorillonite clay nanocomposites prepared by electron beam irradiation

Safaa G. Abd Alla, Reham H. Helal & Abdel Wahab M. El-Naggar

To cite this article: Safaa G. Abd Alla, Reham H. Helal & Abdel Wahab M. El-Naggar (2015) Characterization of poly(vinyl alcohol)/acrylamide/alkylammonium montmorillonite clay nanocomposites prepared by electron beam irradiation, Advanced Composite Materials, 24:1, 41-56, DOI: 10.1080/09243046.2013.871178

To link to this article: http://dx.doi.org/10.1080/09243046.2013.871178

Advanced Composite Materials, 2015
Vol. 24, No. 1, 41–56, http://dx.doi.org/10.1080/09243046.2013.871178

Taylor & Francis
Taylor & Francis Group

Characterization of poly(vinyl alcohol)/acrylamide/alkylammonium montmorillonite clay nanocomposites prepared by electron beam irradiation

Safaa G. Abd Alla, Reham H. Helal and Abdel Wahab M. El-Naggar*

Radiation Chemistry Department, National Center for Radiation Research and Technology, P.O. Box 29 Nasr City, Cairo, Egypt

(*Received 26 May 2013; accepted 19 August 2013*)

In this work, electron beam radiation was used to form nanocomposite gels based on poly(vinyl alcohol) (PVA), acrylamide (AAm), and alkylammonium montmorillonite organo-clay (S-MMT) in the form of films. X-ray diffraction (XRD) measurements indicated that the organo-clay was aggregated and dispersed in the polymer matrix to form a nanocomposite structure. The results indicated that the introduction of S-MMT clay up to 5% ratio decreased the gel content of PVA/AAm hydrogels; however, it improved the thermal stability to a great extent. The swelling was found to depend on the ratios of AAm in the initial gel composition and irradiation dose. Both PVA/AAm hydrogels and PVA/AAm/S-MMT nanocomposites reached the equilibrium swelling state in water after four hours; however, PVA/AM/S-MMT nanocomposites displayed higher swelling than PVA/AAm gels as demonstrated by applying Fick's law of diffusion. In addition, the equilibrium swelling of PVA/AAm gels and their nanocomposites increased with increasing temperature up to 60 °C.

Keywords: electron beam irradiation; nanocomposites; poly(vinyl alcohol); acrylamide; organo-clay; swelling

1. Introduction

Hydrogels are three-dimensional cross-linked polymeric structures, which are capable of swelling and absorbing large amounts of water or biological fluids without either dissolving or changing their shape to a considerable extent.[1–6]

The naturally occurring sodium montmorillonite clay (MMT) is favorite filler for a wide range of polymer composites.[7] MMT has the ability to exchange ions, and this process has been used for structure modifications necessary for mixing with hydrophobic polymers. MMT exhibits a tendency to agglomerate; thus, in some polymeric matrixes, it forms microcomposites with larger particles. Polymer/MMT clay composites have been reported to exhibit unique properties and lead to environmentally friendly and inexpensive composites. The synthesis and characterization of polymer composites with the inorganic Na-MMT clay have been the topics of many research works in recent years.[8–12]

Special attention has been devoted to sodium MMT modified by organic surfactants, such as long-chain alkylammonium salts (organo-clay), to obtain composites with unique properties. In this respect, copolymers of different compositions

---

*Corresponding author. Email: ab_nagga@yahoo.com have been produced by polymerization of various acrylic compounds (e.g. N-isopropylacrylamide (NIPAAm), acrylamide (AAm), and acrylic acid (AAc)).[13] It was found that the swelling stability of the gels was enhanced by the addition of the filler Na-MMT and Na-MMT hydrophobized with alkyl ammonium ions. The extent of swelling was found to be controllable through the hydrophilicity of the initial monomers. Pure AAm gels swelled 30–50-fold, while pure NIPAAm gels swelled 6–12-fold of their dry mass. For the AAm/NIPAAm ratios of 100/0–80/20 the extent of swelling decreased by 16.8 g/g, while in the ratio range of 20/80–50/50 it remained linear. In the molar ratios of 50/50–20/80, the swelling of the gels decreased by a further 16.5 g/g. In the case of NIPAAm-AAc-based copolymers, the 100% AAc-based polymer swelled 35–73-fold. Increasing the molar ratio of AAc resulted in a decrease in swelling. Starting from AAc/NIPAAm molar ratio of 80/20, the decrease was linear and a 10% change in molar ratio in NIPAAm monomer resulted in an average decrease in swelling of 10 g/g. The swelling of the copolymers of the two hydrophilic monomers AAm and AAc, that is, poly(AAm-co-AAc) revealed that the best swelling gels were those that contained 50% each of AAm and AAc. Swelling of the copolymer of this composition was 110- to 120-fold the dry mass of the samples. A series of composites and nanocomposite hydrogels were synthesized by the copolymerization reaction of partially neutralized acrylic acid (SA) with sodium hydroxide solution on bentonite micro powder (BT) using N,N'-methylenebisacrylamide (MBA) as a cross-linker and potassium persulfate as an initiator in aqueous solution.[14] The influences of Na^+BT, organo-BT (O-BT), and the content of the BT in the copolymer gels on the swelling behavior in deionized water and saline solution (0.2 wt.% NaCl) were investigated. The results showed that the equilibrium swelling was decreased by adding a small amount of the BT; however, at higher BT contents, the equilibrium swelling increased with an increase in the amount of clay.

The present work was undertaken to use electron beam irradiation to form nanocomposites based on poly(vinyl alcohol)/acrylamide copolymer hydrogels loaded with low contents (1–5 wt.%) of alkylammonium montmorillonite clay. The main objective was to enhance the thermal stability and swelling characteristics of these nanocomposites.

2. Experimental

2.1. *Materials*

The sodium MMT used in this study has a cation-exchange capacity of 74.6 mequiv/100 g and was supplied by the International Co. for Mining Inc, (ICMI), Egypt. The poly(vinyl alcohol) (PVA) used in this study was of laboratory grade; it was a fully hydrolyzed polymer in the form of powder, with average molecular weight of 106,000, and was purchased from Laboratory Rasayan, Egypt. Acrylamide monomer (AAm) was purchased from BDH Chemicals Co., England. Hexadecyl trimethyl ammonium bromide (HTAB), chemical formula is $C_{19}H_{42}BrN$) was purchased from Aldrich, Germany, and used for the preparation of the organo-montmorillonite clay.

2.2. *Synthesis of organo-montmorillonite (S-MMT)*

Sodium montmorillonite clay (Na-MMT) was first purified by repeated washing cycles with distilled water and filtration. The suspension was then sonicated in an ultrasonic bath for 60 min, allowed to stand overnight, filtered and left to dry in vacuum oven. For the synthesis of organo-montmorillonite filler, 0.01 mol HTAB was dissolved in 250 ml of equal amounts of ethanol and water mixture (pH = 4.0), the solution was added to 10% of Na-MMT swollen in distilled water in 100 ml distilled water, and the system was stirred for 24 h at room temperature. After the completion of ion exchange, the suspension was centrifuged, washed with distilled water, and filtered. The filtrate obtained was dried and ground to 200 μm particle size.

2.3. Synthesis of PVA/AAm/S-MMT nanocomposites

The synthesis of PVA/AAm hydrogel was carried out by dissolving separately (0.9 or 0.8 g) of PVA polymer and (0.1 or 0. 2 g) of AAm monomer in 5 ml distilled water at 80 °C. The hydrogel composition of PVA and AAm in the mixtures was 90/10 and 80/20%. The PVA and AAm solutions were then mixed and stirred to a homogenous mixture. The PVA/AAm/S-MMT nanocomposites were prepared by dispersing various ratios 1–5 wt% (based on the total polymer) in the PVA/AAm solution mixtures with continuous stirring for 15 min; the suspension was then poured into glass dishes (5 cm in diameter). The solutions were made oxygen free by purging nitrogen gas for 5 min and sealed. The solutions were then exposed to different doses of electron beam irradiation at room temperature to obtain polymerized cross-linked films of thickness ~3 mm. Electron beam irradiation was carried out in the electron accelerator (1.5 MeV and 37.5 kW) facility of the National Center for Radiation Research and Technology, Cairo, Egypt. Compositions of the various samples are given in Table 1.

2.4. Gel content determination

Samples of the prepared gel films were first washed with distilled water to remove unreacted materials and impurities, dried, and then accurately weighed (W_o). The dried samples were extracted with distilled water using a Soxhlet system for 6 h to remove soluble parts, dried in a vacuum oven at 50 °C to constant weight (W_1). The gel content was calculated according to the following equation: equation:

$$\text{Gel content } (\%) = (W_1/W_o) \times 100$$

2.5. X-ray diffraction analysis

X-ray diffraction (XRD) characterization of the samples was performed at room temperature with a Philips PW 1390 diffractometer (30 kV, 10 mA), (Netherlands), with Cu-Kα irradiation at a scanning rate of 8°/min in a 2θ range of 4°–90°.

Table 1. Effects of electron beam dose and S-MMT ratio on the gel contents (%) of different ratios of PVA/AAm hydrogels.

	Gel content (%)							
	PVA/AAm (90/10%)				PVA/AAm (80/20%)			
Dose (kGy)	None	S-MMT (1%)	S-MMT (3%)	S-MMT (5%)	None	S-MMT (1%)	S-MMT (3%)	S-MMT (5%)
20	93	55	70	93	95	62	73	95
30	95	60	72	95	98	67	75	98
40	99	64	74	99	100	72	80	100

2.6. Thermogravimetric analysis

Thermogravimetric analysis (TGA) study was carried out on Shimadzu-30 (TGA-30) at a heating rate of 10 °C/min under nitrogen atmosphere from room temperature to 600 °C. The initial TGA data were used to determine the different kinetic parameters of thermal decomposition reaction. The derivative of the TGA thermograms (DTGA) or the rate of reaction (dw/dt) was determined by taking the weight loss every 2 min. The rate of reaction dw/dt was plotted against temperature from which the different kinetic parameters in terms of T_{onset}, T_{endset} , and T_{peck} temperatures can be determined.

2.7. Swelling measurements

Swelling was determined gravimetrically by immersing a dry weight (W_2) of gel films (5 cm in diameter and 0.3 thick) in distilled water for different time intervals up to 24 h at room temperature. The samples were removed at each time interval and blotted on filter paper to remove the excess water on the surface and weighed (W_3). The percentage swelling was calculated according to the following equation:

$$\text{Swelling }(\%) = [(W_3 - W_2)/W_2] \times 100$$

The effect of temperature on the equilibrium swelling was also studied, in which a dry weight of gel (W_4) was immersed in distilled water at different temperatures (10–60 °C) for 24 h. The sample was removed at each temperature and blotted on filter paper to remove the excess water on the surface and weighed (W_T). The swelling (%) at each temperature was calculated as follows:

$$\text{Swelling }(\%) = [(W_T - W_4)/W_4] \times 100$$

3. Results and discussion

3.1. Gel content

Table 1 shows the effect of electron beam irradiation dose and S-MMT ratio on the gel content for the two samples of PVA/AAm hydrogels. The gel content of the PVA/AAm hydrogels increased slightly with increasing irradiation dose up to 40 kGy, irrespective of the two hydrogel compositions. The increase in irradiation dose is associated with increasing the number of free radicals formed on the backbones of chains. The gel content of PVA/AAm hydrogels also increased slightly with increasing the ratio of AAm monomer in the initial preparation. This can be explained on the basis of G(X), which is the number of polymer cross-link sites per 100 eV. The AAm monomer has higher G (X) compared to that for PVA. The gel content was found to decrease greatly by using 1% S-MMT organo-clay and then increased with increasing the content of S-MMT up to 5%. The effect of S-MMT organo-clay on gel contents may be explained as follows: When low contents were used, the S-MMT clay would be best dispersed in the PVA/AAm hydrogel solutions and in turn the active sites may be isolated and will not be accessible to electron beam irradiation and thus a decrease in gel contents was obtained. When higher contents of S-MMT up to 5% were used, the S-MMT nanoparticles would be aggregated in the network structure of hydrogels, as a result of increasing the concentration of dispersion so that the active sites will be more accessible to electron beam irradiation and thus led to an increase in gel content.

3.2. XRD analysis

Depending on the nature of the components used (clay mineral, organic cation, and polymer matrix) and the method of preparation, three main types of composites may be obtained when a clay mineral is combined with a polymer.[15] When the polymer is unable to be intercalated, a phase separated composite is obtained, whose properties stay in the same range as those of traditional microcomposites. In this case, the wide angle X-ray scan of the polymer composite is expected to look essentially the same as that obtained for the organo-clay powder; there is no shifting of the X-ray d-spacing. Generally, such scans are made over a low range of angles, 2θ, such that any peaks from a crystalline polymer matrix are not seen since they occur at higher angles >10°. An intercalated structure is obtained when one or more polymer chains are intercalated between the silicate layers; it results in a well-ordered multilayer morphology built up of alternating polymeric and inorganic layers. When the individual silicate layers are completely and uniformly dispersed in a continuous polymer matrix, an exfoliated or delaminated structure is obtained.[16–18] For completely exfoliated organo-clay, no small angle X-ray peak is expected for the nanocomposite since there is no spacing of the platelets and the distances between platelets would, in any case, be larger than what ordinary X-ray scattering can detect.

Figure 1 shows the XRD patterns of pure MMT clay and the hydrogels based on pure PVA and different ratios of PVA/AM, prepared at a dose of 20 kGy of electron beam irradiation. The XRD patterns of pure organo-clay (S-MMT) and PVA/AAm hydrogels of different compositions loaded with different contents of organo-clay (S-MMT) prepared at the same dose are shown in Figures 2 and 3. The XRD parameters of the strongest peaks of the different compositions are summarized in Table 2. As shown in Figure 1, the XRD pattern of pure MMT clay showed a basal of 6.510 Å (12.5° 2θ) spacing between ordered layers, in which water expanded the sodium clay. The XRD pattern of the S-MMT organo-clay showed a strong peak at $2\theta = 5.61°$, corresponding to a basal spacing of 15.74 Å. This indicates that the organo-clay layers were separated by the surfactant octadecylammonium ions.

As shown in Figures 2 and 3, the XRD peak, corresponding to S-MMT, no longer occurs. The XRD peaks of copolymer hydrogels of PVA/AAm loaded with organo-clay were located at higher 2θ ($2\theta > 5$) and appeared as broad peaks. This indicates that the polymers were not intercalated and a phase separated composite was obtained, whose properties stay in the same range as those of traditional microcomposites. The organo-clay is thus aggregated and dispersed in the polymer matrix. The XRD peaks for the 10% AAm-based copolymer hydrogel were wider than those for the 20% AAm-based copolymer hydrogel (higher gel content). This may be explained based on the higher cross-linking, which occurred after dispersion, and would eventually make the platelets more compact.

3.3. Thermogravimetric analysis

The dissociation energies of the covalent bonds C–H, C–C, C=O, C–O, O–H, N–H, and C–N were reported to be 414, 347, 741, 351, 464, 389, and 293 kJ/mol, respectively.[19] According to these values, the average complete dissociation energy (ACDE) for PVA and PAAm can be calculated as follows:

For PVA [–$(CH_2CH–OH)_{n}$–] = C–H (3X414) + C–C (1X347) + C–O (1X351) + O–H (1x464) = 2404/6 = 400.7 kJ/mol.

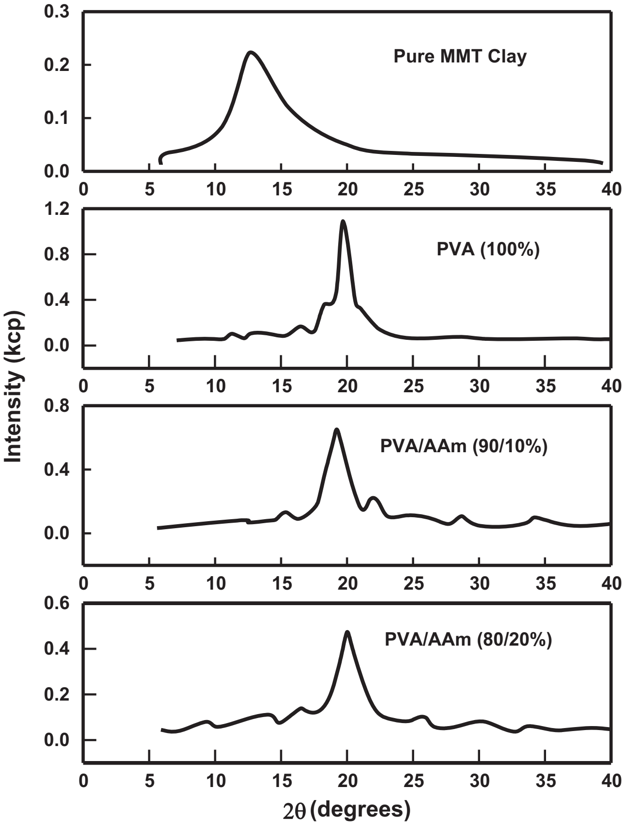

Figure 1. XRD patterns of pure MMT clay and the hydrogels based on pure PVA and different ratios of PVA/AAm, prepared at a dose of 20 kGy of electron beam irradiation.

For PAAm [–(CH_2–$CHCONH_2$)$_n$] = C–H (3X414) + C–C (2X347) + C=O (1X741) + C–N (1x293) + N–H (1X389) = 3359/8 = 419.9 kJ/mol.

According to these calculations, few points may be indicated: (1) Even though PAAm molecule contains a weak C–N bond, which will dissociate first, it contains a strong C=O bond, which resist thermal dissociation. (2) In the average, PAAm with ACDE (419.9 kJ/mol) would resist thermal dissociation than PVA with ACDE of 400.7 kJ/mol. (3) In conclusion, it may be expected that the formation of hydrogels with increased AAm ratio will theoretically improve the thermal stability of PVA/AAm hydrogels. TGA was used to investigate experimentally the effect of electron beam dose, AAm ratio, and S-MMT content on the thermal stability of the different composites formed at various doses. Figure 4 shows the TGA thermograms and the corresponding rate of thermal decomposition reaction (d*w*/d*t*) for the PVA/AAm (90/10%) hydrogel loaded with different ratios of S-MMT clay, prepared at the 20 kGy dose of electron beam irradiation (as representative). The residual weight (%) at different heating temperatures and the kinetic temperatures of the thermal decomposition for all the composites prepared at different doses are summarized in Table 3. Based on the results in this Table, few points can be summarized:

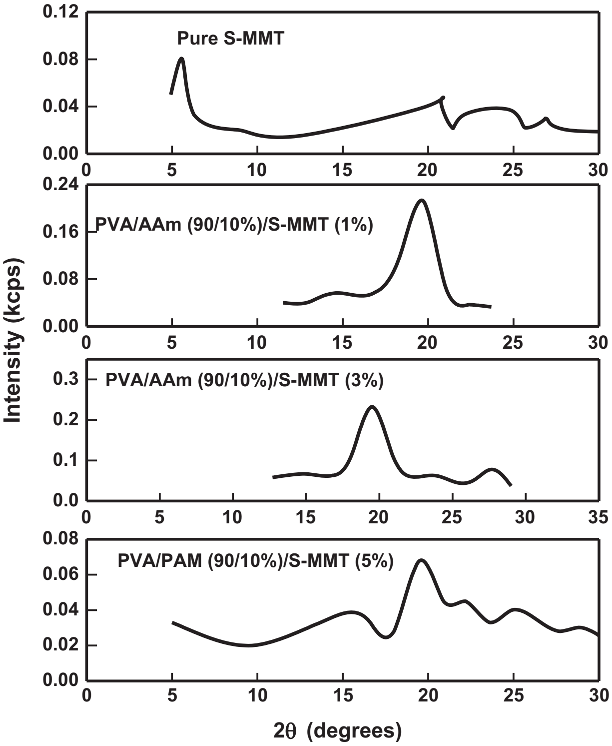

Figure 2. XRD patterns of pure S-MMT clay and PVA/AAm (90/10%) hydrogels loaded with different ratios of S-MMT, all were prepared at a dose of 20 kGy of electron beam irradiation.

(1) Up to a heating temperature of 600 °C, the PVA/AAm copolymer hydrogels had higher thermal stability, with higher residual weight (%), than PVA hydrogel. The thermal stability of the PVA/AAm copolymer hydrogels increased with increasing the ratio of AAm, in which the residual weight (%) for the PVA/AAm (80/20%) was higher than that for PVA/AAm (90/10%), regardless of irradiation of dose.

(2) The effects of S-MMT nanoparticles and dose on the thermal stability of PVA/AAm copolymer hydrogel differed from composition to another. Up to a heating temperature of 500 °C, the thermal stability, based on residual weight (%), of PVA/AAm (90/10%) hydrogels, prepared at the 20 kGy dose, decreased with increasing the content of S-MMT up to 3% and then tended to increase at 5%. Similar trends were observed for the same composition prepared at the 40 kGy dose. Further heating up to 600 °C of the same hydrogel composition, the thermal stability decreased with increasing both S-MMT content and dose. For the PVA/AAm (80/20%) hydrogels, the thermal stability increased with increasing the content of S-MMT up to 5% within the temperature up to 600 °C, regardless of dose. In conclusion, both PVA/AAm/S-MMT compositions had the same thermal stability when a 5% of S-MMT clay was used and prepared at the 20 kGy dose. It is clear that the determination of thermal stability according to the residual weight (%) is difficult.

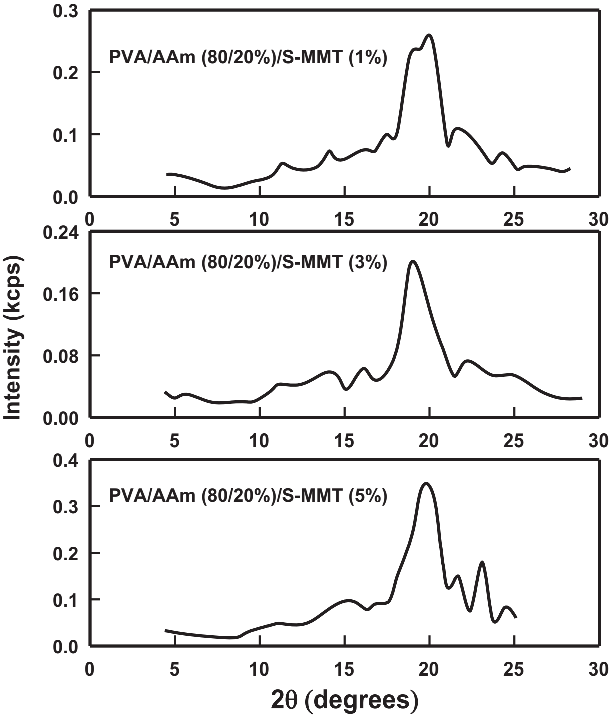

Figure 3. XRD patterns of PVA/AAm (80/20%) hydrogels loaded with different ratios of S-MMT, all were prepared at a dose of 20 kGy of electron beam irradiation.

Table 2. Summary of XRD patterns of pure MMT clay, pure S-MMT clay, pure PVA, pure PVA/AAm hydrogels, and PVA/AAm/S-MMT composites, prepared at the 20 kGy dose of electron beam irradiation.

PVA/AAm composites	2θ (degrees)	D (Å)	Intensity (kcps)
Pure MMT clay	12.741	6.510	0.224
Pure S-MMT organo-clay	5.609	15.740	0.080
PVA (100%)	19.647	4.499	1.089
PVA/AAm (90/10%)	19.038	4.658	0.592
PVA/AAm/S-MMT (90/10/1%)	19.718	4.499	0.213
PVA/AAm/S-MMT (90/10/3%)	19.548	4.537	0.233
PVA/AAm/S-MMT (90/10/5%)	19.888	4.461	0.060
PVA/AAm (80/20%)	19.944	4.537	0.477
PVA/AAm/S-MMT (80/20/1%)	20.228	4.386	0.248
PVA/AAm/S-MMT (80/20/3%)	18.868	4.699	0.193
PVA/AAm/S-MMT (80/20/5%)	19.548	4.537	0.335

(3) As shown from Figure 4(A), the TGA thermograms for all the hydrogels of PVA, PVA/AAm, and PVA/AAm/S-MMT composites displayed multithermal decomposition stages; the first was from room temperature up to 300 °C, the second, represents the major thermal decomposition, was from 300 to 450 °C, and the third was from 450 to 600 °C. As shown in Figure 4(B), the rate of thermal decomposition reactions displayed similar

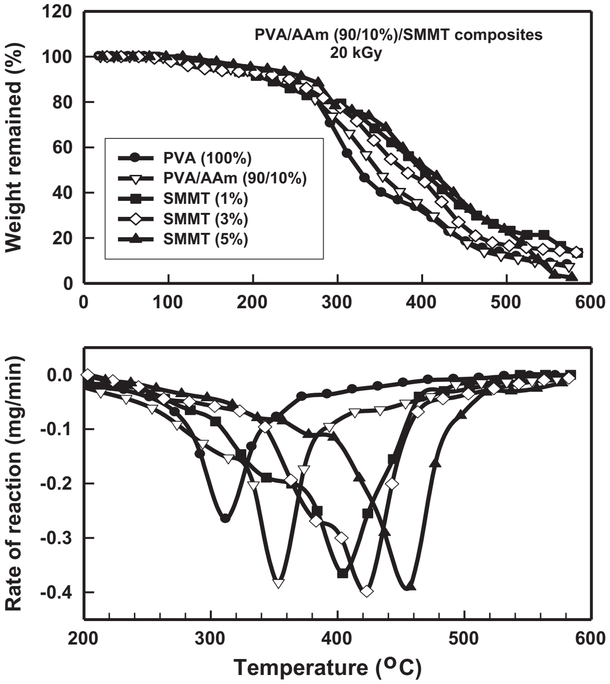

Figure 4. TGA thermograms and rate of thermal decomposition reaction of the hydrogels of pure PVA and PVA/AAm (90/10%), before and after loading with different ratios of S-MMT, all were prepared at a dose of 20 kGy.

trends; however the maximum temperature of the rate of reaction (T_{peak}) differed from one material to another. A single T_{peak} was observed for PVA/AAm copolymer hydrogels or their composites with S-MMT clay indicating compatibility between components; otherwise, a multi T_{peak} was seen if there were non-compatible components. According to the values of T_{peak}, it can be concluded that the increase in S-MMT content in the initial preparation solutions increased the thermal stability to a high degree as shown in Table 3. This may be explained since the introduction of organo-clay will introduce additional organic covalent bonds with higher dissociation energies.

(4) The different kinetic temperatures (T_{onset} and T_{endset}) indicated that the thermal stability of the two copolymer hydrogels were both higher than that of the PVA hydrogel as shown in Table 3. The introduction of organo-clay resulted in a further improvement in the thermal stability. This is additional evidence that the S-MMT layers were homogenously dispersed in the polymer matrix, although with different levels of dispersion. The improvement of thermal stability can be attributed to the barrier effect of S-MMT. S-MMT is a layered structure and small molecules generated during thermal decomposition process cannot permeate and thus have to bypass.[20]

Table 3. Residual weight (%) at different heating temperatures and the temperatures of thermal decomposition parameters of PVA and PVA/AAm/S-MMT composites, prepared at 20 and 40 kGy doses of electron beam irradiation.

PVA/AAm/ S-MMT ratios (%)	Dose (kGy)	Residual weight (%) 500 °C	Residual weight (%) 600 °C	T_{onset} (°C)	T_{endset} (°C)	T_{peak} (°C)
100/0/0	20	11.8	8.2	255	385	312
	40	11.5	8.2	286	354	318
90/10/0	20	12.2	7.5	314	391	353
	40	20.4	7.5	330	392	372
90/10/1	20	23.2	13.4	343	460	404
	40	19.4	10.3	314	461	414
90/10/3	20	16.6	13.7	363	461	423
	40	13.0	13.0	310	458	427
90/10/5	20	23.8	12.6	397	498	457
	40	14.3	11.8	311	514	449
80/20/0	20	13.1	10.8	338	452	390
	40	29.5	9.0	343	436	392
80/20/1	20	14.5	7.7	419	490	450
	40	14.7	8.6	368	496	452
80/20/3	20	14.2	11.1	415	516	452
	40	18.8	13.7	396	499	454
80/20/5	20	23.3	13.9	424	505	472
	40	14.5	12.0	443	523	476

3.4. Swelling studies

The effect of electron beam dose on the swelling-time dependency in water at 25 °C of pure PVA and PVA/AAm copolymer hydrogels is shown in Figure 5, while the effect of electron beam dose on the swelling-time dependency of the different nanocomposites of PVA/AAm/S-MMT loaded with different ratios of S-MMT is shown in Figures 6 and 7.

Based on these Figures, two conclusions can be made:

(1) The swelling of all the copolymer hydrogels or their composites with organo-clay increased progressively within the initial time of swelling up to four hours and then tended to level off and reaches the equilibrium state. The swelling decreased with increasing the ratio of AAm monomer in the initial solutions for the same irradiation dose due to the higher gel content of PAAm than PVA. The swelling, however, decreased with increasing irradiation dose for the same copolymer composition as shown in Figure 5. This may be explained based on the increase in irradiation dose would increase the cross-linking density, which causes the structure to be more compact and thus decrease the swelling.

(2) The swelling of PVA/AAm/S-MMT composites depended largely on the ratio of organo-clay, in which the swelling increased with increasing the content of organo-clay due to the highly dispersed organo-clay in the network. As shown in Figures 6 and 7, the introduction of S-MMT clay had effects on swelling. Thus, the structure of PVA/AAm/S-MMT composites is neither exfoliated nor intercalated.

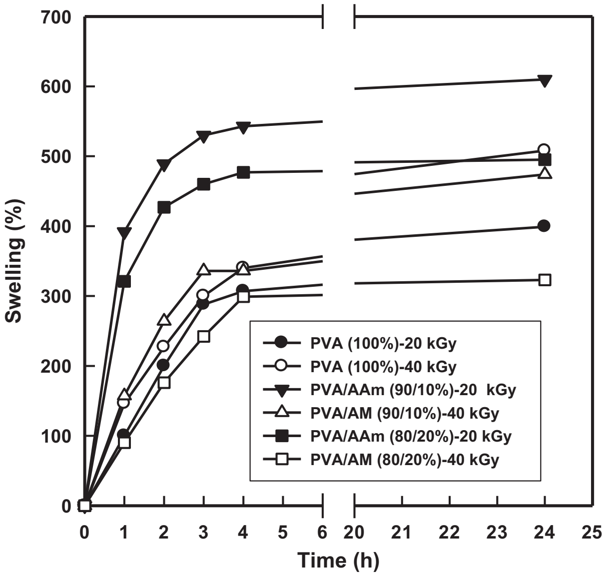

Figure 5. Swelling kinetics in water at 25 °C and pH 7 of different hydrogels prepared at different doses of electron beam irradiation.

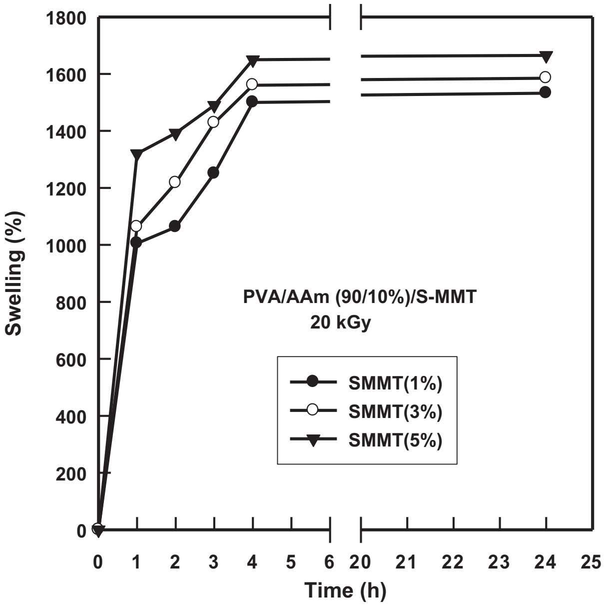

Figure 6. Swelling kinetics in water at 25 °C and pH 7of PVA/AAm (90/10%) hydrogels loaded with different contents of S-MMT clay, prepared at a dose of 20 kGy of electron beam irradiation.

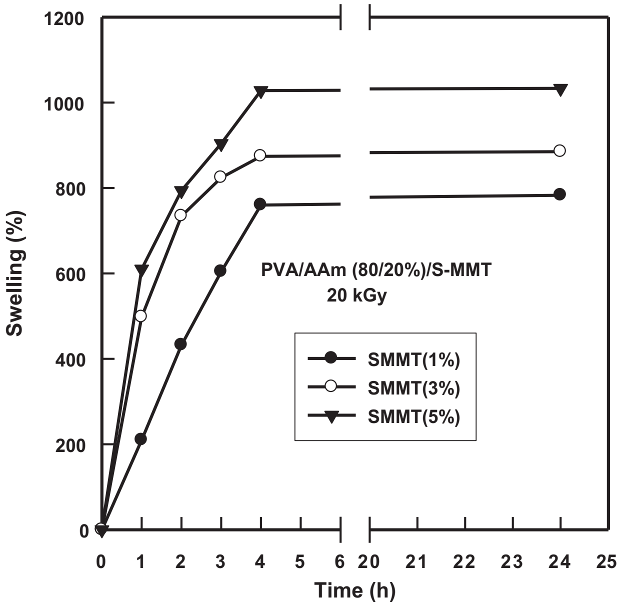

Figure 7. Swelling kinetics in water at 25 °C and pH 7 of PVA/AAm (80/20%) hydrogels loaded with different contents of S-MMT clay, prepared at a dose of 20 kGy of electron beam irradiation.

To obtain a more quantitative understanding of the nature of the water diffusion kinetics in the PVA/AAm/S-MMT composites, the initial swelling data were fitted to the following exponential heuristic equation:[21]

$$F = M_t/M_e = kt^n \text{ or } \ln k + n \ln t$$

where M_t is the amount of water absorbed by the hydrogel at time t, M_e is the amount of water absorbed at equilibrium, k is a constant characteristic of the macromolecular network system and n is the diffusion exponent, which is indicative of the transport mechanism. When ln F is plotted against ln t, it gives a straight line from which the intercept determines the constant k and the slope gives the exponent n. Based on the relative rate of diffusion of water into polymer matrix and rate of polymer chain relaxation, swelling of polymers has been classified into three types of diffusion mechanisms.[22,23] These mechanisms are Case I simple Fickian diffusion, Case II diffusion, and Case III Non-Fickian or anomalous diffusion. Simple Fickian diffusion is characterized by $n = 0.5$, while case II diffusion is characterized by $n = 1$ and Non-Fickian diffusion is characterized by 'n' between 0.5 and 1.0.[22,23] Figure 8 shows the application of the above equation to the PVA/AAm (90/10%)/S-MMT composites (as representative). The calculations of the diffusion parameters of all the composites are listed in Table 4. Based on the data on Table 4, few points can be addressed as follows: (1) The two samples of PVA/AAm copolymer hydrogels displayed a different Fickian diffusion types. The PVA/AAm (90/10%) displayed a non-Fickian diffusion type (n between 0.29 and 0.58), in which the diffusion of water into the hydrogel networks is not controlled but it depends on water sorption process, which in turn depends on the structure and pathways of water through the networks. The PVA/AAm (80/20%) displayed a

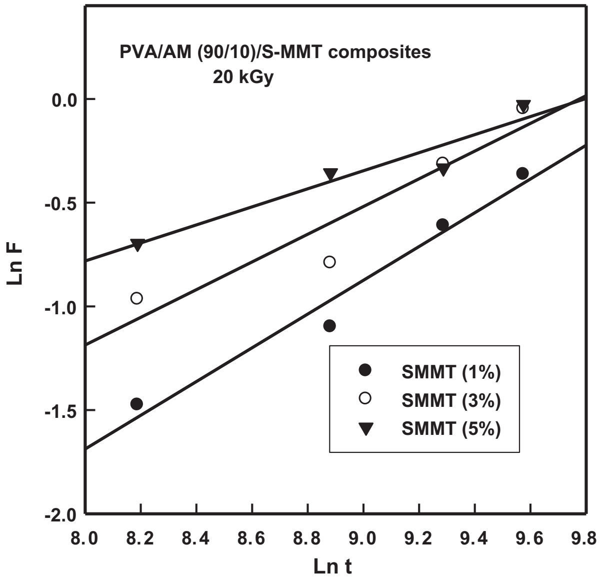

Figure 8. Plots of ln F against ln t of the PVA/AAm (90/10%) hydrogels, loaded with different ratios of S-MMT. All were prepared at a dose of 20 kGy of electron beam irradiation.

Table 4. Summary of water diffusion kinetic parameters of PVA/AAm/S-MMT composites, prepared at different doses of electron beam irradiation.

PVA/AAm/SMMT ratios (%)	EB dose (kGy)	*n*	*k*
90/10/0	20	0.29	0.6679
	40	0.58	0.3127
90/10/1	20	0.24	0.6556
	40	0.62	0.2895
90/10/3	20	0.81	0.2156
	40	1.00	0.5429
90/10/5	20	0.67	0.3462
	40	0.59	0.9916
80/20/0	20	0.93	0.4492
	40	1.31	1.1342
80/20/1	20	1.01	0.3776
	40	1.20	1.2823
80/20/3	20	1.11	0.3127
	40	1.43	0.9451
80/20/5	20	0.93	0.4492
	40	1.31	1.1342

simple Fickian diffusion type (*n* between 0.93 and 1.31), in which the diffusion of water into the hydrogel networks is controlled, regardless of dose. (2) The PVA/AAm (90/10%)/S-MMT composites displayed a non-Fickian diffusion type (*n* between 0.24 and 0.59). However, PVA/AAm (80/20%)/S-MMT composites displayed a simple Fickian diffusion type (*n* between 0.93 and 1.43). The higher *n* and *k* values for the PVA/AAm (90/10%)/S-MMT composites than those for the PVA/AAm/S-MMT (80/20%), at the same irradiation dose, may be attributed to the relatively higher gel con-

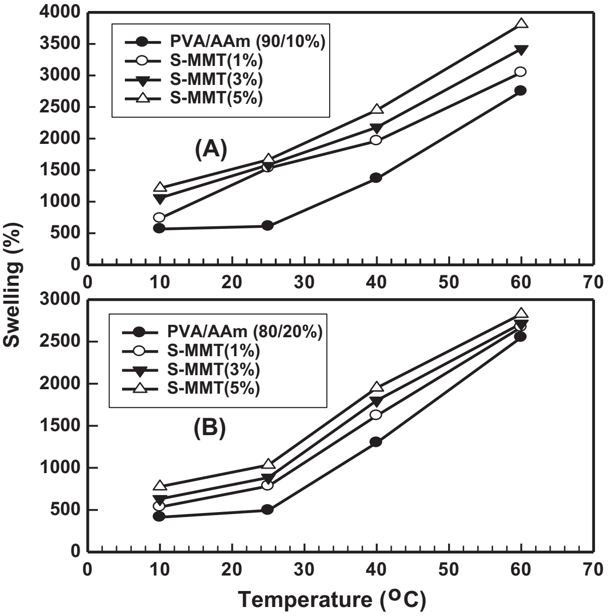

Figure 9. Effect of temperature on the equilibrium swelling of different ratios of PVA/AAm/S-MMT composites PVA/AAm, prepared at the 20 kGy dose of electron beam irradiation.

tent (Table 1), which impede the diffusion of water and in accordance with the swelling kinetics (Figures 6 and 7). It seems that the introduction of S-MMT organo-clay facilitates water diffusion, in which the dispersion of organo-clay nanoparticles creates more resting places for water molecules.

3.5. Effect of temperature on equilibrium swelling

Figure 9 shows the effect of temperature on the equilibrium swelling for PVA/AAm/S-MMT composites, prepared at a dose of 20 kGy of electron beam irradiation. The swelling (%) of all the hydrogel composites increased with increasing temperature up to 60 °C with different trends. While the swelling of the PVA/AAm (90/10%)/S-MMT composite increased progressively with increasing temperature from 25 to 60 °C (Figure 9(A)), there is no noticeable increase in swelling of the PVA/AAm (80/20%)/S-MMT from 10 to 25 °C and then it increased progressively from 25 to 60 °C (Figure 9(B)). It is clear that the swelling of PVA/AAm (90/10%)/S-MMT composite is faster than PVA/AAm (80/20%)/S-MMT. In addition, the swelling increased with increasing the content of S-MMT in the initial solutions, regardless of composition and temperature. This increase in the swelling with increasing temperature may be explained as follows. At higher temperatures, the free volume of the gels is increased resulting in increasing the mobility of chains and hence facilitates the diffusion of water molecules from the surroundings.

4. Conclusions

In this work, the effect of composition, irradiation dose, organo-clay content, and temperature on the swelling of PVA/AAm copolymer hydrogels loaded with organo-clay nanoparticles was studied. The results indicated that the dose and AAm ratio played an important role on swelling. In general, the increase in dose and AAm ratio was accompanied with a decrease in swelling due to increased cross-linking density. Swelling of the hydrogels increased significantly with increasing the content of S-MMT organo-clay. The data indicated that all the copolymer hydrogels displayed a non-Fickian type of diffusion, in which the diffusion of water into the hydrogel networks is anomalous. However, the PVA/AAm (90/10%)/S-MMT composites displayed a simple Fickian diffusion type. The XRD measurements indicated that a phase separated composite was obtained, whose properties stay in the same range as those of traditional microcomposites. TGA implied that introduction of organo-montmorillonite clay into the polymer hydrogels networks led to an increase in their thermal stability.

References

[1] Emileh A, Vasheghani-Farahani E, Imani M. Swelling behavior, mechanical properties and network parameters of pH- and temperature-sensitive hydrogels of poly((2-dimethyl amino) ethyl methacrylate-co-butyl methacrylate). Eur. Polym. J. 2007;43:1986–1995.

[2] Mahdavinia GR, Zohuriaan-Mehr MJ, Pourjavadi A. Modified chitosan III, superabsorbency, salt- and pH-sensitivity of smart ampholytic hydrogels from chitosan-g-PAN. Polym. Adv. Technol. 2004;15:173–180.

[3] Benoit DSV, Nuttelman CR, Collins SD, Anseth KS. Synthesis and characterization of a fluvastatin-releasing hydrogel delivery system to modulate hMSC differentiation and function for bone regeneration. Biomaterials. 2006;27:6102–6110.

[4] Coughlan DC, Corrigan OI Drug-polymer interactions and their effect on thermoresponsive poly(N-isopropylacrylamide) drug delivery systems. Int. J. Pharm. 2006;313:163–174

[5] Abd Alla SG, Kandeel MM, El-Naggar AM. Characterization of hydrogels prepared by the γ-irradiation of aqueous solutions of acrylamide and N-vinyl-2-pyrrolidone comonomers. J. Appl. Polym. Sci. 2007;106:4202–4208.

[6] Abd Alla SG, Nizam El-Din HM, El-Naggar AM. Structure and swelling-release behaviour of poly(vinyl pyrrolidone) (PVP) and acrylic acid (AAc) copolymer hydrogels prepared by gamma irradiation. Eur. Polym. J. 2007;43:2987–2998.

[7] Kaczmarek H, Podgórski A. The effect of UV-irradiation on poly(vinyl alcohol) composites with montmorillonite. J. Photochem. Photobiol., A. 2007;191:209–215.

[8] Shibayama M, Suda J, Karino T, Okabe S, Takehisa T, Haraguchi K. Structure and dynamics of poly(N-isopropylacrylamide)-clay nanocomposite gels. Macromolecules. 2004;37:9606–9612.

[9] Haraguchi K, Li HJ. Mechanical properties and structure of polymer–clay nanocomposite gels with high clay content. Macromolecules. 2006;39:1898–1905.

[10] Lee WF, Chen YC. Effects of intercalated hydrotalcite on drug release behavior for poly (acrylic acid-co-N-isopropyl acrylamide)/intercalated hydrotalcite hydrogels. Eur. Polym. J. 2006;42:1634–1642.

[11] Haraguchi K, Li HJ, Matsuda K, Takehisa T, Elliott E. Mechanism of forming organic/inorganic network structures during *in-situ* free-radical polymerization in PNIPA-clay nanocomposite hydrogels. Macromolecules. 2005;38:3482–3490.

[12] Miyazaki S, Karino T, Endo H, Haraguchi K, Shibayama M. Clay concentration dependence of microstructure in deformed poly(N-isopropylacrylamide)-clay nanocomposite gels. Macromolecules. 2006;39:8112–8120.

[13] Janovak L, Varga J, Kemeny L, Dekany I. Swelling properties of copolymer hydrogels in the presence of montmorillonite and alkylammonium montmorillonite. Appl. Clay Sci. 2009;43:260–270.

[14] Santiago F, Mucientes AE, Osorio M, Rivera C. Preparation of composites and nanocomposites based on bentonite and poly(sodium acrylate). Effect of amount of bentonite on the swelling behaviour. Eur. Poly. J. 2007;43:1–9.

[15] Paul DR, Robeson LM. Polymer nanotechnology: nanocomposites. Polymer. 2008;49:3187–3204.

[16] Alexandre M, Dubois P. Polymer-layered silicate nanocomposites: preparation, properties and uses of a new class of materials. Mater. Sci. Eng. 2000;28:1–63.

[17] Smarsly B, Garnweitner G, Assink R, Brinker CJ. Preparation and characterization of mesostructured polymer-functionalized sol–gel-derived thin films. Prog. Org. Coat. 2003;47:393–400.

[18] Haraguchi K, Li HJ, Matsuda K, Takehisa T, Elliott E. Mechanism of forming organic/inorganic network structures during *in-situ* free-radical polymerization in PNIPA-clay nanocomposite hydrogels. Macromolecules. 2005;38:3482–3490.

[19] Whitten KW, Gailelt KD. General chemistry with quantitative analysis. Philadephia: Saunders College Publishing; 1981. p. 372.

[20] Liu Z, Zhou P, Yan D. Preparation and properties of nylon-1010/montmorillonite nanocomposites by melt intercalation. J. Appl. Polym. Sci. 2004;91:1834–1841.

[21] Peppas NA, Gurny R, Doelker E, Buri D. Modelling of drug diffusion through swellable polymeric. J. Membr. Sci. 1980;7:241–253.

[22] Ritger PL, Peppas NA. A simple equation for description of solute release I. Fickian and non-fickian release from non-swellable devices in the form of slabs, spheres, cylinders or discs. J. Controlled Release. 1987;5:23–36.

[23] Ritger PL, Peppas NA. A simple equation for description of solute release II. Fickian and anomalous release from swellable devices. J. Controlled Release. 1987;5:37–42.